# Electron gas and hydrogen:
## from ground state energies to excitation spectra

Markus Holzmann
LPMMC, CNRS UGA Grenoble

- Ground state energies:
  iterated backflow, neural network wave functions

- Energy gaps (insulators):
  single particle excitations (charged gap)
  particle-hole excitations (neutral gap)

- Fermi liquid properties (metals):
  momentum distribution
  renormalization factor Z
  effective mass m*

# Born-Oppenheimer approximation

- Non-relativistic Hamiltonian for ions and electrons

$$H = -\sum_n \frac{\hbar^2 \nabla_n^2}{2M} - \sum_i \frac{\hbar^2 \nabla_i^2}{2m} + \sum_{n<m} \frac{e^2}{|\mathbf{r}_i - \mathbf{r}_j|} - \sum_{n,i} \frac{Ze^2}{|\mathbf{r}_i - \mathbf{R}_n|} + \sum_{n<m} \frac{Z^2 e^2}{|\mathbf{R}_n - \mathbf{R}_m|}$$

$$= -\sum_n \frac{\hbar^2 \nabla_n^2}{2M} + H_e(\mathbf{R})$$

- Born-Oppenheimer approximation ($T \ll T_F$): electronic ground state for fixed ion positions

$$H_e(\mathbf{R})\Psi(\mathbf{r}) = E_0(\mathbf{R})\Psi(\mathbf{r})$$

- Density matrix/ distribution of ions

$$\rho(\mathbf{R}) = \left\langle \mathbf{R} \left| e^{-H/T} \right| \mathbf{R} \right\rangle \simeq \left\langle \mathbf{R} \left| \exp\left\{ -\left[ -\sum_n \frac{\hbar^2 \nabla_n^2}{2M} + E_0(\mathbf{R}) \right] /T \right\} \right| \mathbf{R} \right\rangle$$

# Coupled Electron-Ion Monte Carlo (CEIMC)

C. Pierleoni, D.M. Ceperley, M. H., Phys. Rev. Lett. 93, 146402 (2004)

- Use QMC methods for electronic Born-Oppenheimer ground state energies

$$E_0(\mathbf{R}) \leq \frac{\int d\mathbf{r}\Psi_T(\mathbf{r})H_e(\mathbf{R})\Psi_T(\mathbf{r})}{\int d\mathbf{r}\Psi_T^2(\mathbf{r})}$$

- Sample classical ion distribution

$$\rho(\mathbf{R}) \propto e^{-E_0(\mathbf{R})/T}$$

- Path-Integral Monte Carlo for quantum nuclei

$$\rho(\mathbf{R}) \propto \int \mathbf{R}_1 \cdots \int \mathbf{R}_{P-1} \langle \mathbf{R}|e^{-\beta H/P}|\mathbf{R}_1\rangle\langle \mathbf{R}_1|e^{-\beta H/P}|\mathbf{R}_2\rangle \cdots \langle \mathbf{R}_{P-1}|e^{-\beta H/P}|\mathbf{R}\rangle$$

$$\propto \int \mathbf{R}_1 \cdots \int \mathbf{R}_{P-1} \exp\left[-\sum_p \left(\frac{M(\mathbf{R}_{p-1}-\mathbf{R}_p)^2}{2\hbar^2\beta/P} + \beta E_0(\mathbf{R}_p)/P\right)\right]$$

CEIMC: all distributions sampled by Monte Carlo methods

**Alternative approch:**

use **molecular (Langevin) dynamics** to sample classical ion distribution

C. Attaccalite and S. Sorella, Phys Rev. Lett. 100, 114501 (2008).

# CEIMC: Some challenges

➔ Precise electronic wave functions:

$$\mathbf{q}_i = \mathbf{r}_i + \sum_{j \neq i} (\mathbf{r}_j - \mathbf{r}_i)\eta(|\mathbf{r}_j - \mathbf{r}_i|)$$

Slater-Jastrow

$$\Psi_{SJ}(\mathbf{R}) = \det_{\mathbf{k}i} \phi_{\mathbf{k}}(\mathbf{r}_i) \exp\left[-U_2\right]$$

$$U_2 = \sum_{i<j} u_2(\mathbf{r}_i - \mathbf{r}_j)$$

Backflow - 3body

$$\Psi_{bf3}(\mathbf{R}) = \det_{\mathbf{k}i} \phi_{\mathbf{k}}(\mathbf{q}_i) \exp\left[-U_2 - U_3\right]$$

$$U_3 = \lambda \sum_i \left[\sum_{j \neq i} (\mathbf{r}_i - \mathbf{r}_j)\nu(\mathbf{r}_i - \mathbf{r}_j)\right] \left[\sum_{j \neq i} (\mathbf{r}_i - \mathbf{r}_j)\nu(\mathbf{r}_i - \mathbf{r}_j)\right]$$

How to generalize wave functions to closer to exact electronic ground state?

- Thermodynamic limit extrapolation needed → Size consistency!

  → Search for minimal set of parameters, check with DMC/RMC….

➔ Electronic properties: Excitation spectra...

➔ Exploring phase diagram: simulations of very large systems needed
without prior knowledge of phases, unit cells (NPT,...)

→ Machine learned effective proton-proton potential

H. Niu, Y. Yang, S. Jensen, M. H., C. Pierleoni, D.M. Ceperley, Phys. Rev. Lett. 130, 076102 (2023)

# ➔Exploring phase diagram:

Machine learned effective proton-proton potential

H. Niu, Y. Yang, S. Jensen, M. H., C. Pierleoni, D.M. Ceperley, Phys. Rev. Lett. 130, 076102 (2023)

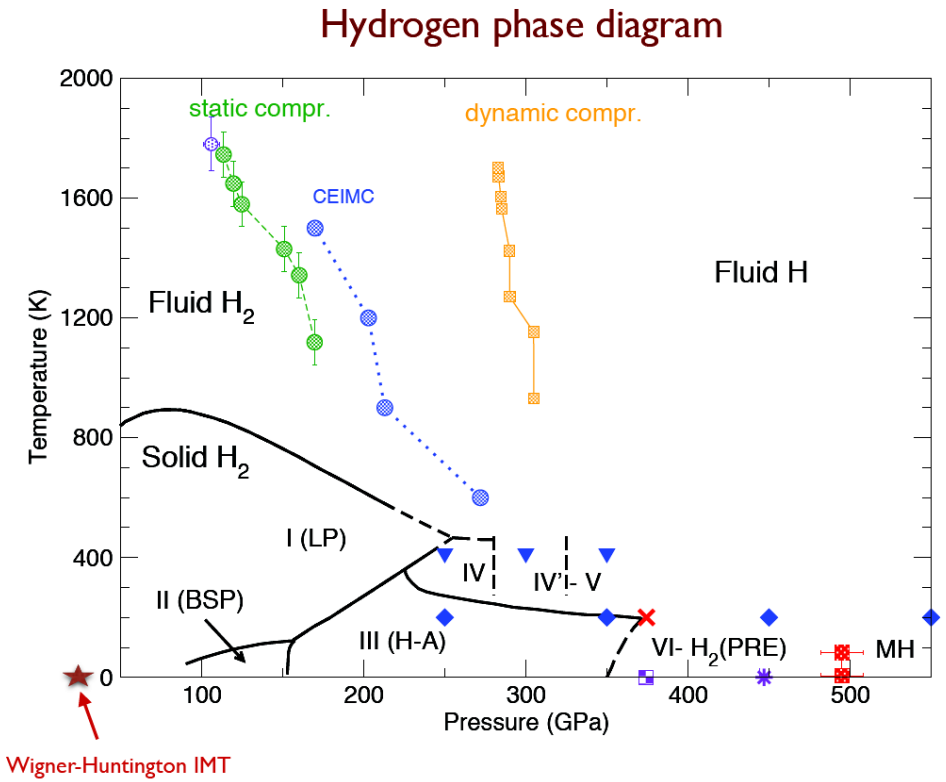


Pierleoni, Morales, Rillo, Holzmann, Ceperley PNAS 113, 4953 (2016)

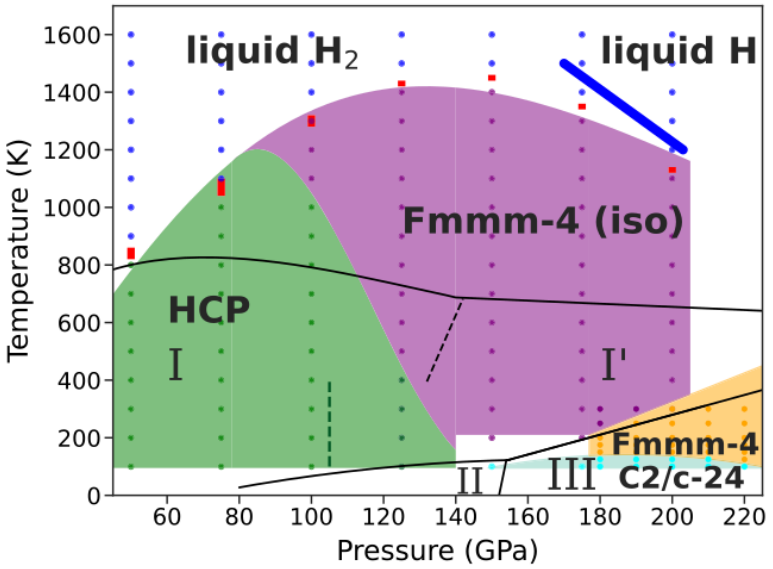


FIG. 1. Phase diagram of dense hydrogen. The dots indicate the ($P$, $T$) values where we ran PIMD simulations using a DMC-trained DPMD interatomic potential. Colors indicate the identified phase: dark blue (liquid), green (HCP), purple ($Fmmm$-4 isotropic), orange ($Fmmm$-4 oriented), and cyan ($C2/c$-24). The vertical green dashed line at 105 GPa indicates a crossover within HCP to an in-plane orientation. The thick blue line is the estimate of the transition from liquid $H_2$ to liquid H from Ref. [10]. Red bars are estimates of the melting temperature from two-phase coexistence simulation. The black lines are experimental estimates of phase boundaries, solid lines for the melting, dashed line for I-I′ transition [39].

# Trial wave functions: Many-body correlations ($U_n$ with n>2)

- Analytical forms/ efficient calculations:

- Most general 3body form $U_3(\mathbf{R}) = \sum_{i<j<k} u_3(\mathbf{r}_{ij}, \mathbf{r}_{ik})$

- Local energy method suggests

$$U_3[\mathbf{R}] = \sum_i \sum_{j,k} \mathbf{r}_{ij} \cdot \mathbf{r}_{ik} u_3(r_{ij}) u_3(r_{ik}) = \sum_i \left[ \sum_j \mathbf{r}_{ij} u_3(r_{ij}) \right] \cdot \left[ \sum_k \mathbf{r}_{ik} u_3(r_{ik}) \right]$$

- Introduce generalized vector/tensor forms

"backflow vector" $\mathbf{d}_i = \sum_{j \neq i} \mathbf{r}_{ij} d(r_{ij})$ → 1D functions to be optimized

"backflow tensor" $\underline{T}_i|_{\alpha\beta} = \sum_{j \neq i} \mathbf{r}_{ij}|_\alpha \mathbf{r}_{ij}|_\beta t(r_{ij})$ $\alpha = x, y, z$

- **n-body correlations** must be scalars:

$U_3 = \lambda \sum_i \mathbf{d}_i \cdot \mathbf{d}_i$ $U_4 = \sum_i \mathbf{d}_i \cdot \underline{T}_i \cdot \mathbf{d}_i$

**n-body backflow** $\mathbf{x}_i = \underline{T}_i \mathbf{d}_i$

M.H., Bernu, Ceperley, Phys. Rev. B 74, 104510 (2006)

- easily automatized
- Chain rules for derivatives
- 1D function per vector/tensor
- Computational cost remains ~ $N^2$

# Strongly inhomogeneous systems (electrons in atoms): Orbital backflow

M. H. and S. Moroni, Phys. Rev. B 99, 085121 (2019)

VMC

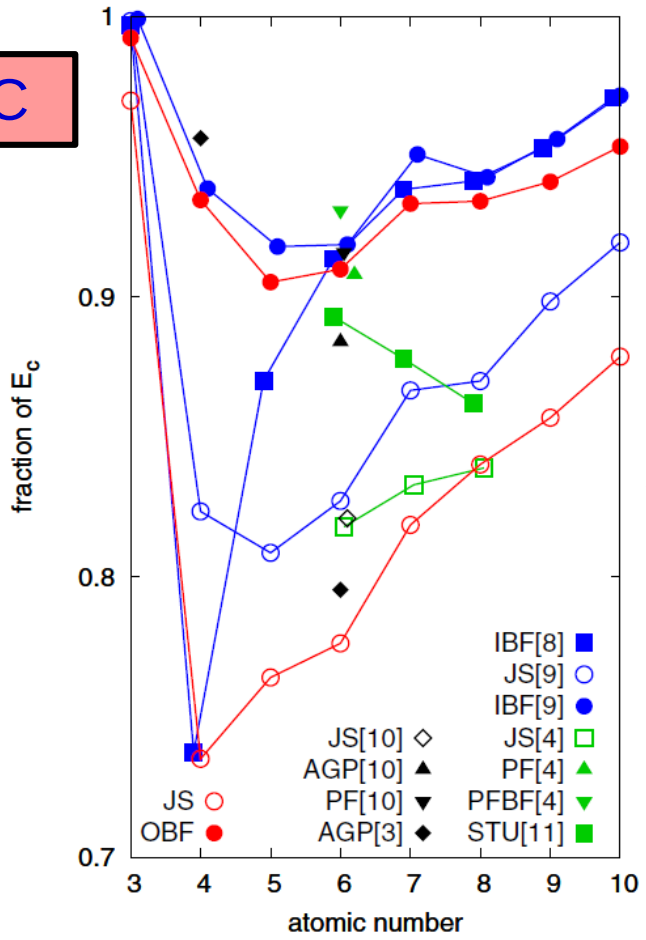


FIG. 1. Fraction of correlation energy recovered in VMC for the first row atoms of orbital backflow wave functions (OBF) compared to previous results using different kinds of single-determinant wave function, namely antisymmetrized geminal product (AGP) [3,10], Pfaffian (PF) [4], inhomogeneous backflow (IBF) [8,9], Pfaffian including inhomogeneous backflow (PFBF) [4], and a general Pfaffian form dubbed STU [11]. Empty symbols denote the bare Slater-

Couple orbitals in Slater-determinant via many-body correlations

$$\phi_n(\mathbf{r}_i) \longrightarrow \phi_n^{(1)}(\mathbf{r}_i) + (\mathbf{q}_i(X) - \mathbf{r}_i) \cdot \nabla \phi_n^{(2)}(\mathbf{r}_i)$$

=> lattice version of backflow:

Tocchio, Becca, Parola, Sorella, Phys. Rev. B 78, 041101(R) (2008)
Luo, Clark, Phys. Rev. Lett. 122, 226401 (2019)

**Single Determinant wfns**

DMC

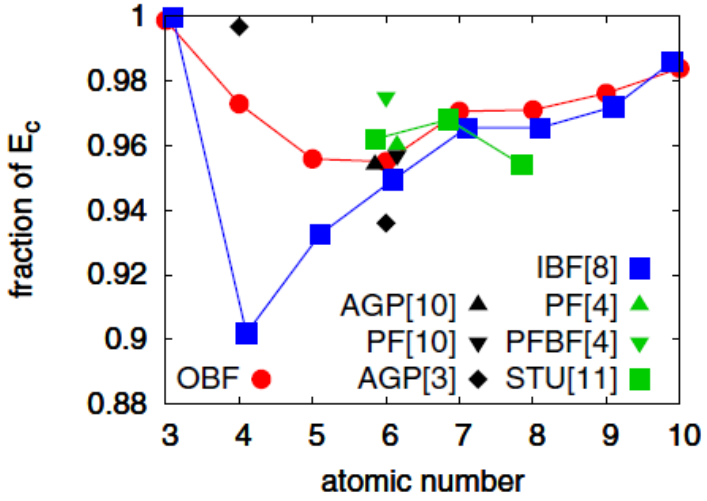


FIG. 2. Fraction of correlation energy recovered in fixed-node DMC for the first row atoms of orbital backflow wave functions (OBF) compared to previous results of different kinds of single-determinant wave functions. Notations are the same as those of

# Trial wave functions: Iterative backflow renormalization

M.Taddei, M. Ruggeri, S. Moroni, M.H., Phys. Rev. B 91, 115106 (2015)

- Start with basis set of single particle Slater determinants

$$\Psi_{\mathbf{K}}^{(0)} = \det_{\mathbf{k}\in\mathbf{K},i} e^{i\mathbf{k}\cdot\mathbf{r}_i}$$

  and consider Hamiltonian matrix elements

$$H_{\mathbf{K},\mathbf{K}'} = \left\langle \Psi_{\mathbf{K}}^{(0)} \left| H \right| \Psi_{\mathbf{K}'}^{(0)} \right\rangle$$

- Determine "canonical" transformation to **approximately diagonalize** Hamiltonian
  Bohm, Pines, Phys. Rev. 92, 609 (1953)

$$\Psi_{\mathbf{K}}^{(1)} \sim e^{-S}\Psi_{\mathbf{K}}^{(0)}$$

=> Jastrow potential sums up effective 2-particle collissions (+ *plasmons*)
backflow eliminates weak momentum dependence (plasmon-electron interaction)

M. H., Ceperley, Pierleoni, Esler, Phys. Rev. E 68, 046707 (2003)

$$\Psi_{\mathbf{K}}^{(1)} \sim \det_{\mathbf{k}\in\mathbf{K},i} e^{i\mathbf{k}\cdot\mathbf{q}_i^{(1)}(\mathbf{R})} \times \exp\left[-U^{(1)}(\mathbf{R})\right]$$

$$U^{(1)}(\mathbf{R}) = \sum_{i<j} u_2^{(1)}(r_{ij})$$

$$\mathbf{q}_i^{(1)} = \mathbf{r}_i + \sum_{j\neq i} \mathbf{r}_{ij}\eta^{(1)}(r_{ij})$$

- Effective Hamiltonian within correlated backflow wave functions

$$H_{\mathbf{K},\mathbf{K}'}^{(1)} = \left\langle \Psi_{\mathbf{K}}^{(1)} \left| H \right| \Psi_{\mathbf{K}'}^{(1)} \right\rangle$$

approximate diagonalization

$$\Psi_{\mathbf{K}}^{(2)} \sim \det e^{i\mathbf{k}\cdot(\mathbf{q}_i^{(1)}+\mathbf{q}_i^{(2)})} \times \exp\left[-U^{(1)} - U^{(2)}\right]$$

**=> new Jastrow/backflow**

$$U^{(2)}(\mathbf{Q}^{(1)}) = \sum_{i<j} u_2^{(2)}(q_{ij}^{(1)})$$

$$\mathbf{q}_i^{(2)}(\mathbf{Q}^{(1)}) = \sum_{j\neq i} \mathbf{r}_{ij}\eta^{(2)}(q_{ij}^{(1)})$$

$$\mathbf{Q}^{(1)} = (\mathbf{q}_1^{(1)}, \mathbf{q}_2^{(1)}, \ldots, \mathbf{q}_N^{(1)})$$

- Iterate "renormalization" procedure…..

**=> Renormalized Fermi liquid wave functions**

# Backflow network from path integral method

Ruggeri, Moroni, M.H., Phys. Rev. Lett. 120, 205302 (2018).

$$\Psi_\tau(\mathbf{R}) \sim \int d\mathbf{R}' \exp\left[-\lambda(\mathbf{R}-\mathbf{R}')^2 - V(\mathbf{R}) - U(\mathbf{R}')\right]$$

**Perform integration of hidden layers approximately**

by expanding U around some (arbitrary) point Q $\quad U(\mathbf{R}') \approx U(\mathbf{Q}) + (\mathbf{R}'-\mathbf{Q})\nabla U(\mathbf{Q})$

$$\Psi_\tau(\mathbf{R}) \approx \int d\mathbf{R}' \exp\left[-\lambda(\mathbf{R}'-\mathbf{R}+\nabla U/2\lambda)^2 - V(\mathbf{R})\right] \times \exp\left[-U(\mathbf{Q}) - (\mathbf{R}-\mathbf{Q})\cdot\nabla U + (\nabla U)^2/4\lambda\right]$$

choose Q at the center of the gaussian (small τ ≡ large λ)

=> implicit determination of Q by $\quad \mathbf{Q} = \mathbf{R} - \nabla U(\mathbf{Q})/2\lambda \rightarrow \mathrm{q}_i \simeq \mathrm{r}_i - \sum_{j\neq i} \mathrm{r}_{ij}\eta(r_{ij})$

$$\Psi_\tau(\mathbf{R}) \sim \exp\left[-V(\mathbf{R}) - U(\mathbf{Q}) - (\nabla U)^2/4\lambda\right]$$

**and iterate…..**

⇒ **Backflow network**

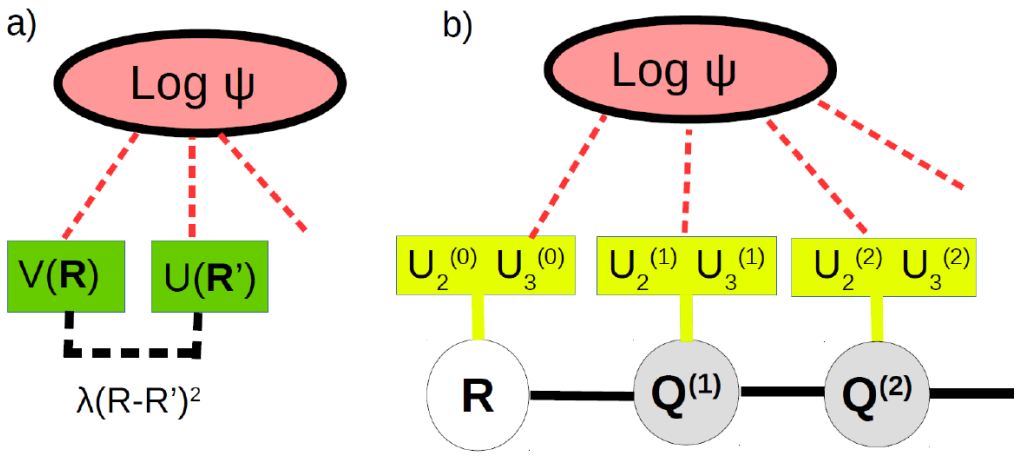


**exponential convergence for "smooth" potentials...**

*fermionic determinants are not smooth….*

# Neural network based wave functions: WAP-net

M. Wilson, S. Moroni, M. H., N. Gao, F. Wudarski, T. Vegge, A. Bhowmik
Phys. Rev. B 107, 235139 (2023).

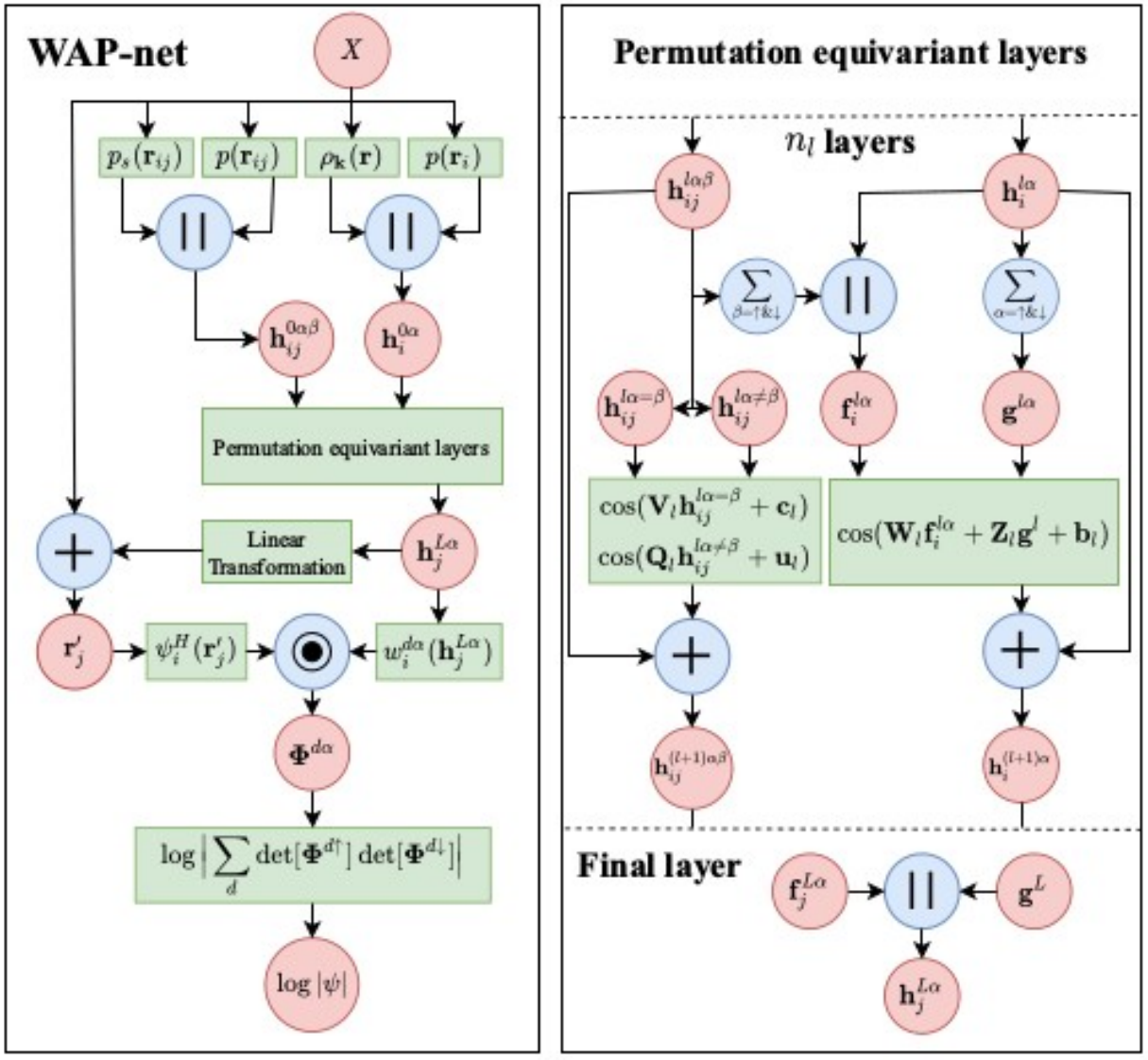

# Benchmark HEG N=14
# IBF, WAP-net, FermiNet, MP-NQS, FCI...

**High density $r_s$<5**

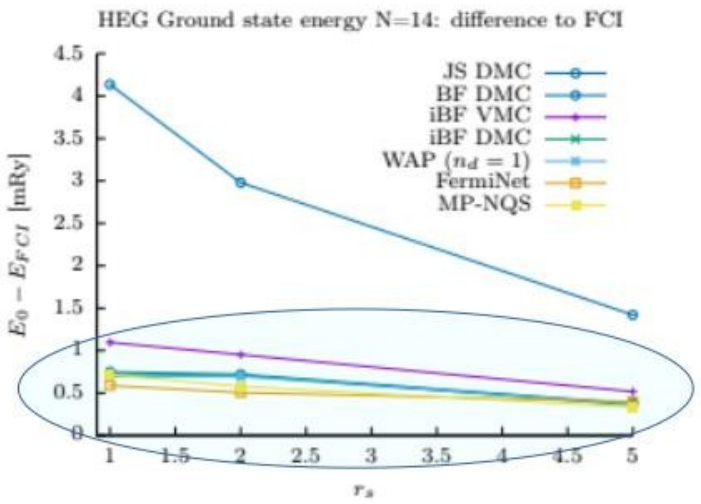


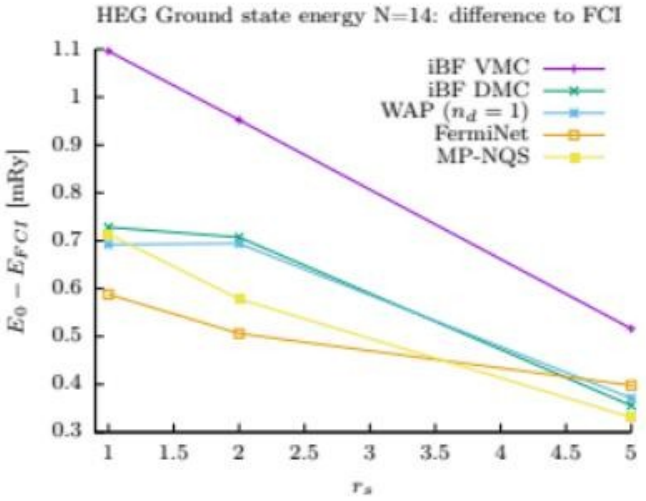


**low density $r_s$>5**

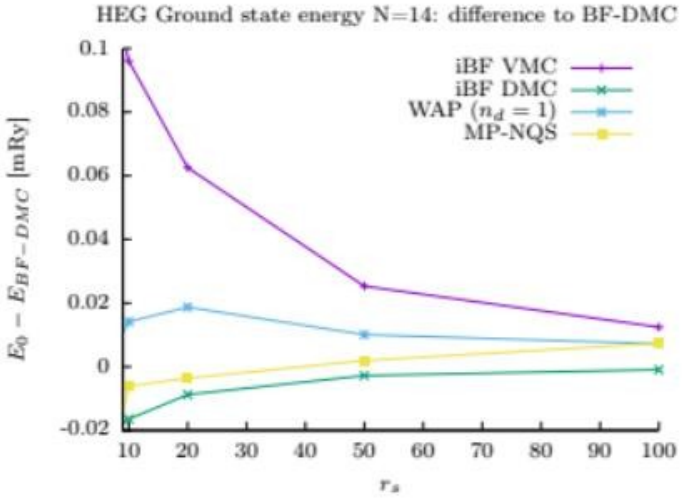


FCI:
K. Liao, T. Schraivogel, H. Luo, D. Kats, A. Alavi,
Phys. Rev. Research 3, 033072 (2021).

FermiNet:
G. Cassella, H. Sutterud, S. Azadi, N. D. Drummond,
D. Pfau, J. S. Spencer, W. M. C. Foulkes,
Phys. Rev. Lett. 130, 036401 (2023).

MP-NQS:
G. Pescia, J. Nys, J. Kim, A. Lovato, G. Carleo,
arXiv 2305.07240 (2023).

# Application of iterated backflow renormalization: Polarization (Stoner) transition in the HEG?

M.H. and S. Moroni, Phys. Rev. Lett. 124, 206404 (2020)

Many-body correlations in the low Density region can be accurately Extrapolated by iterative backflow

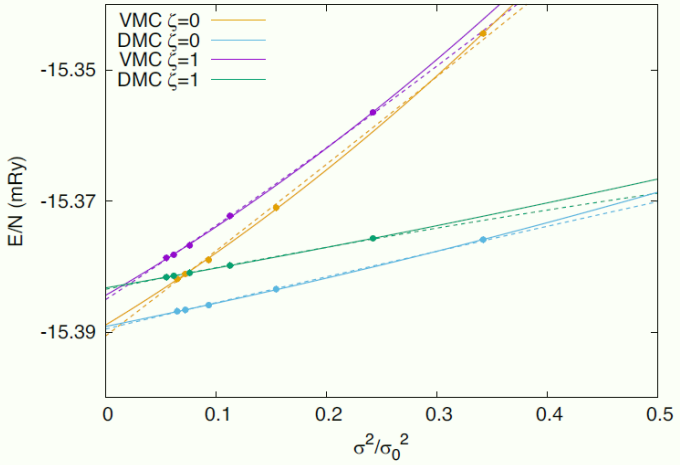


FIG. 1. Extrapolation of the energy to zero variance for $r_s = 100$ at polarizations $\zeta = 0$ and 1. The data are calculated with VMC and DMC using SJ, BF0, …, BF4 wave functions in order of decreasing energy. The reference value $\sigma_0^2$ is the variance of the local energy at $\zeta = 0$ with the SJ wave function. The curves are quadratic fits; for each set of data points (VMC and DMC for $\zeta = 0$ and 1) there are two curves, one of which (solid line) excludes the SJ energy from the fit.

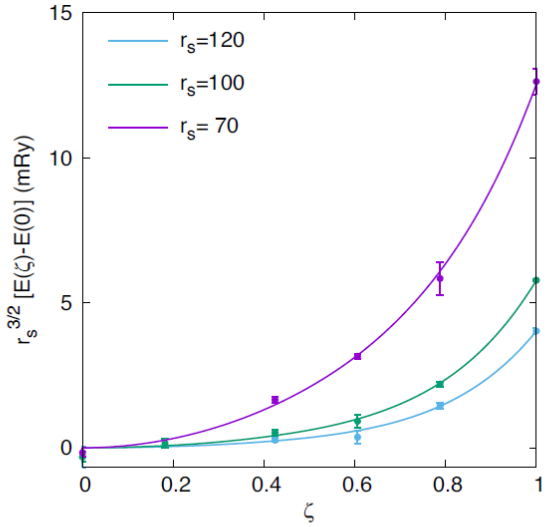


FIG. 3. The polarization energy $E(\zeta) - E(0)$ obtained from zero-variance extrapolations of the DMC energies without the SJ result. The lines are polynomial fits with terms of order 0, 2, and 6. Alternative functional forms and ensuing confidence levels for

Wigner crystalization sets in before Polarization transition

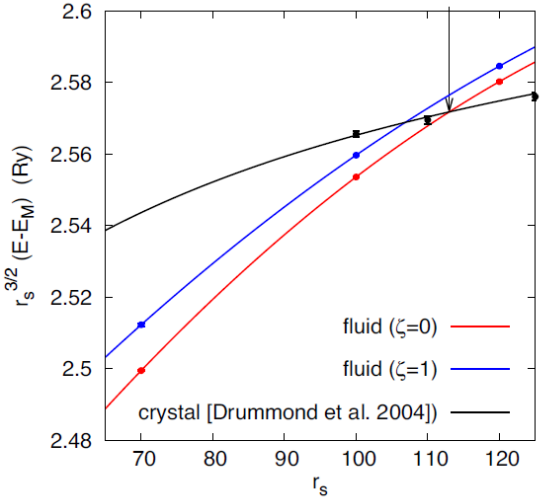

# From ground states to excitations…..

## High pressure hydrogen: Insulator-metal transition

- Characterize insulator: spectral (optical) properties, gaps,...

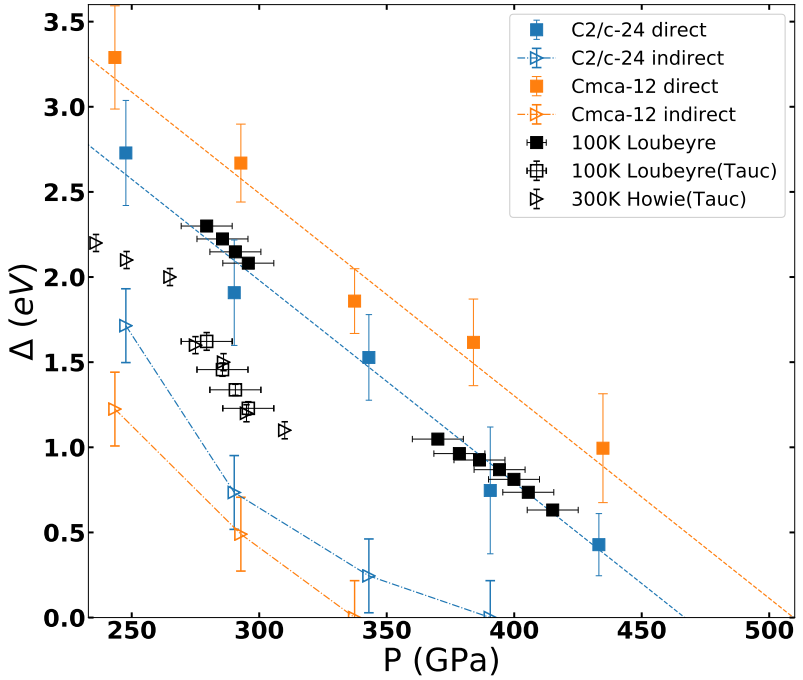


V. Gorelov, M. Holzmann, D. Ceperley, C. Pierleoni, PRL 124, 116401 (2020)

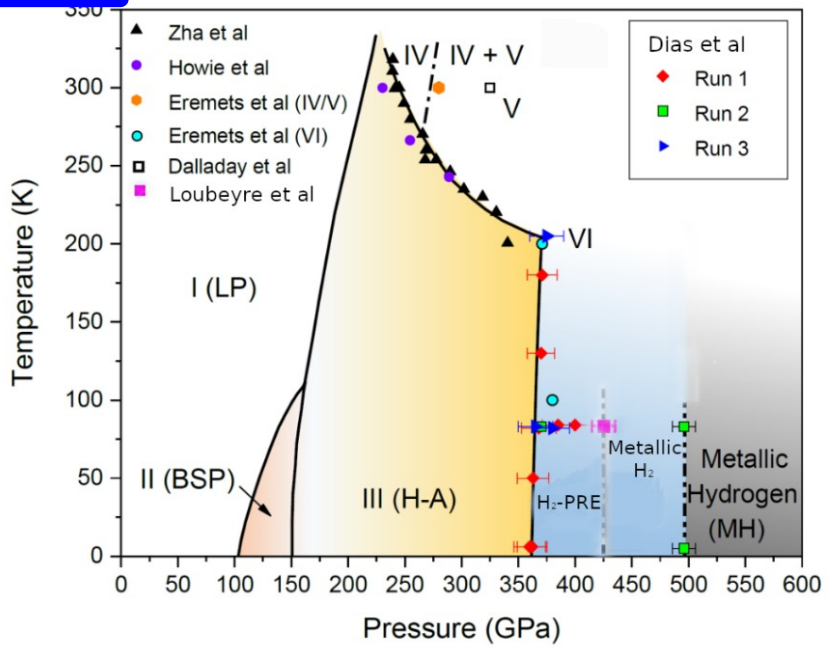


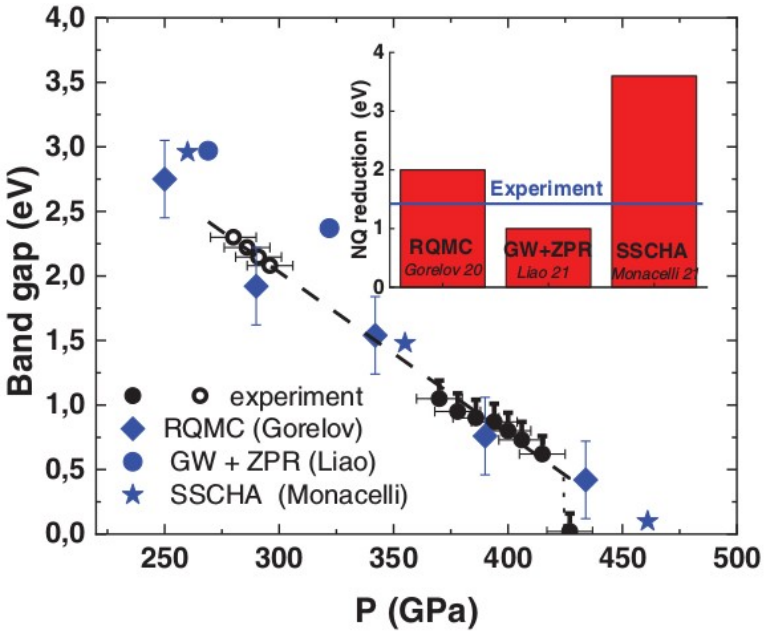


P. Loubeyre, F. Occelli , P. Dumas, PRL 129, 035501 (2022)

# Excitation spectra of insulators (I): single-particle (charge) excitation gap

Y. Yang, V. Gorelov, C. Pierleoni, D. Ceperley, M. H., Phys. Rev. B 101, 085115 (2020)

- consider perfect crystal with fixed number $N_P$ of ions
  add and substract electrons N=…, $N_P$-1, $N_P$, $N_P$+1,… (+ background charge)

$$\Delta = E_0(N_P) + 1 + E_0(N_P - 1) - 2E_0(N_P)$$ (fundamental gap)

contains only ground state energies (variational)

- Impose twisted boundary conditions on wave functions $\Psi(\mathbf{r}_1 + L_x\hat{x}) = e^{i\theta_x}\Psi(\mathbf{r}_1).$

$$f = \frac{1}{M_\theta V}\sum_\theta \min_N \left[E_0(N,\theta) - \mu N\right]$$ ("grand-canonical" N vs μ)

- Can be extended to include nuclear quantum/thermal motion (phonons)

V. Gorelov, D. M. Ceperley, M. H., C. Pierleoni, J. Chem. Phys. 153, 234117 (2020);

- Coulomb size effects

$$\Delta V = \frac{1}{2}\left[\int \frac{d^3\mathbf{k}}{(2\pi)^3} - \frac{1}{V}\sum_{\mathbf{k}\neq 0}\right]\frac{4\pi e^2}{k^2}\left[S(k)-1\right]$$

$$S_k^{\pm} \equiv (N_e \pm 1)S_{N_e\pm 1}(k) - N_e S_{N_e}(k) \qquad \lim_{k\to 0} S_k^{\pm} = \alpha_{\pm} + \mathcal{O}(k^2),$$

- Size effects for gap:

$$\left[\int \frac{d^3k}{(2\pi)^3} - \frac{1}{V}\sum_{\mathbf{k}\neq 0}\right]\frac{v_k}{2}S_k^{\pm} \simeq \alpha_{\pm}\frac{|v_M|}{2} \sim L^{-1} \sim N_e^{-1/3}$$

- General

$$\Delta_\infty - \Delta_V = \frac{|v_M|}{\epsilon} + \mathcal{O}\left(\frac{1}{V}\right)$$

Si diamond (test case)

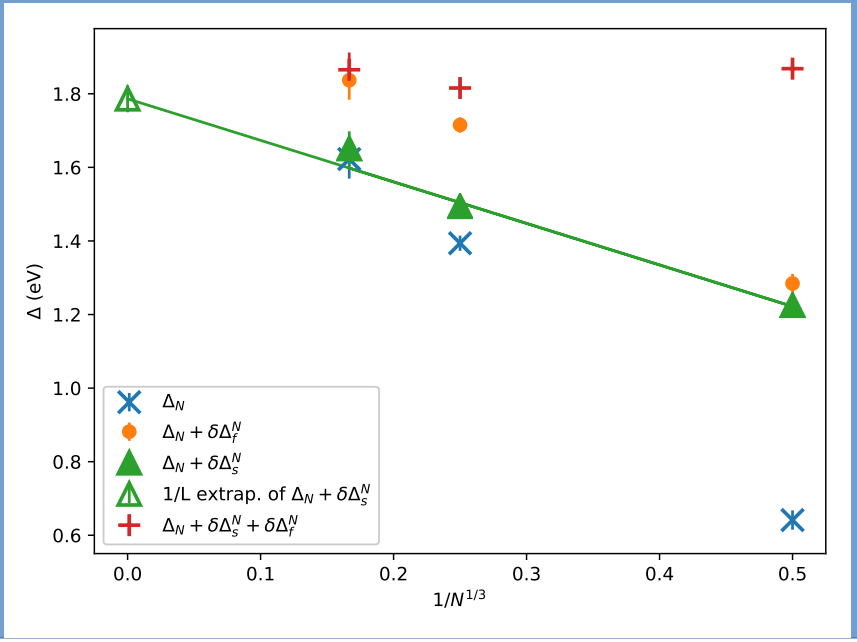


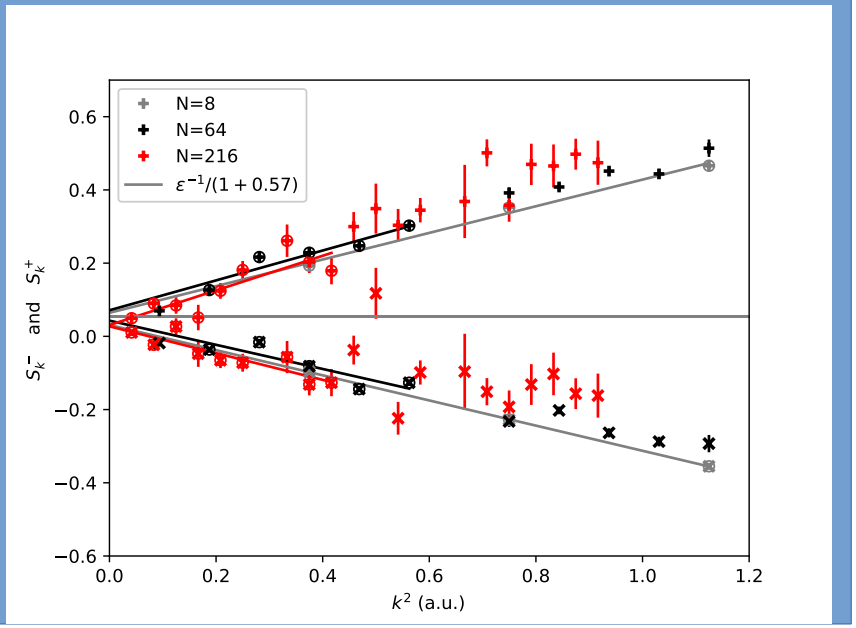

# Excitation spectra of insulators (II): paricle-hole (neutral) excitation gap

V. Gorelov, Y. Yang, M. Ruggeri, D. M. Ceperley, C. Pierleoni, M.H. cond-mat/2303.17944 (2023).

Size effects depend on localized/extended character

- Localized e-h excitation (exciton): $\Delta_\infty - \Delta_N \sim \frac{1}{N}$
- extended e-h excitation (inter-band transitions): $\Delta_\infty - \Delta_N \sim \frac{1}{L} \sim \frac{1}{N^{1/3}}$

Localization of e-h pairs
needs supercells larger to localization length

$$L \gtrsim 2l_x$$

$$l_X \sim \frac{\hbar^2 \epsilon}{m_X e^2}$$

Excitonic size effects can be estimated based on dielectric constant and effective band mass

$$\Delta_n(\infty) - \Delta_n(L) = \frac{|v_M(L)|}{\epsilon} - \frac{|v_M(2l_X)|}{\epsilon}$$

# Hydrogen: Phase I (hcp): electronic gap from QMC vs experiment

V. Gorelov, M.H., D. M. Ceperley, C. Pierleoni, in preparation

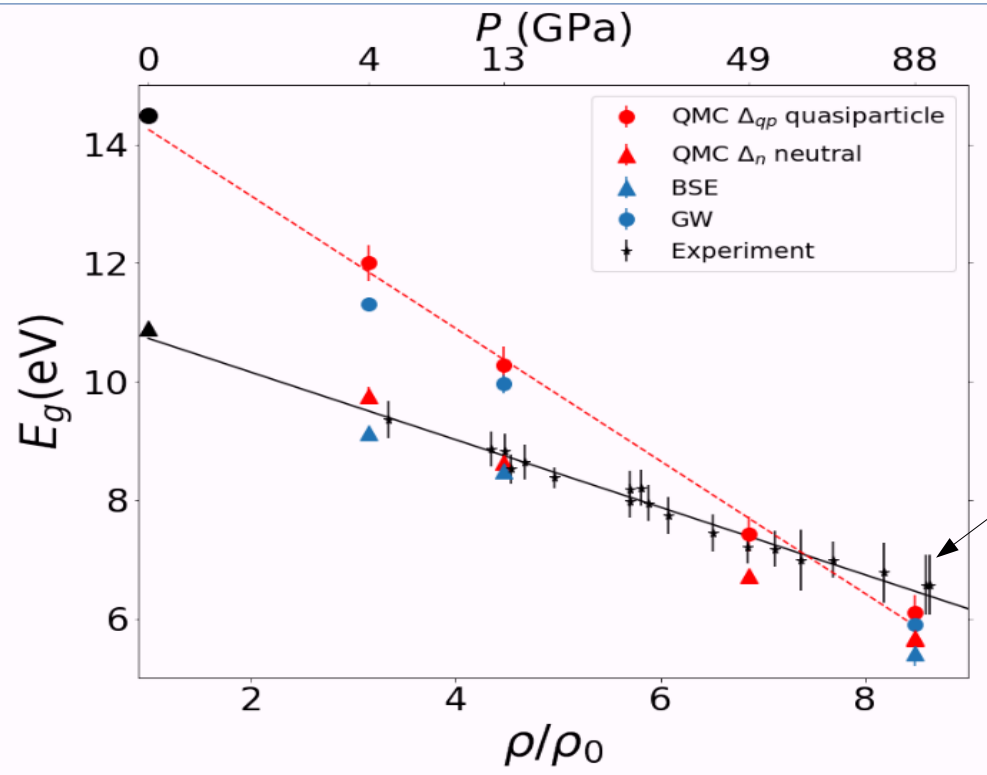


FIG. 1. Comparison between room temperature experimental data and theoretical predictions for the electronic gap of solid hydrogen in phase I as a function of compression. Experimental data are from ref. [16]. We report quasi-particle and neutral gap from QMC (red symbols, quasiparticle circles, neutral triangles) and from MBPT (blue symbols, circles BSE, triangle GW) both corrected for finite size effects. Reference density value $\rho_0$ corresponds to $r_{s_0} = 3.2413$. The continuous line is the fit to experimental data: $E_g(\rho/\rho_0) = 11.3 - 0.57(\rho/\rho_0)$.

Experimental results from inelastic X-ray scattering:

Gap from lower limit of photon energy loss spectra

B. Li, Y. Ding, D. Y. Kim, L. Wang, T.-C. Weng, W. Yang, Z. Yu, C. Ji, J. Wang, J. Shu, J. Chen, K. Yang, Y. Xiao, P. Chow, G. Shen, W. L. Mao, H.-K. Mao, *Probing the Electronic Band Gap of Solid Hydrogen by Inelastic X-Ray Scattering up to 90 GPa,* Physical Review Letters 126, 36402 (2021).

# Landau-Fermi Liquid (I)

Ideal Fermions:

occupation number:
Fermi-Dirac distribution

$$n_{k\sigma} = \frac{1}{e^{(\hbar^2 k^2/2m - \mu)/T} + 1}$$

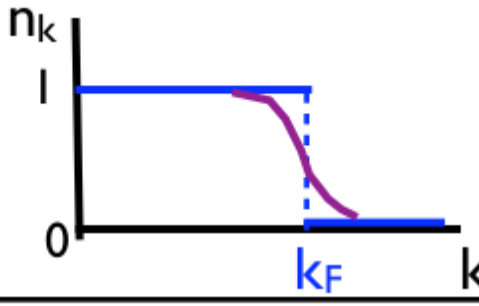


- Observation:

  Low Temperature Properties of a Fermi liquid ($^3$He)

  ≈ ideal Fermi gas with renormalized parameters

- Interacting Fermions postulating quasi-particles:

single particle dispersion with effective mass m*

$$\varepsilon^0_{k\sigma} = \frac{\hbar^2 k_F}{m^*}\left(|\mathbf{k}| - k_F\right)$$

$$E(\delta n_{k\sigma}) = E_0 + \sum_{k,\sigma} \varepsilon^0_{k\sigma}\delta n_{k\sigma} + \frac{1}{2V}\sum_{k\sigma k'\sigma'} f_{k\sigma,k'\sigma'}\delta n_{k\sigma}\delta n_{k'\sigma'} + \ldots$$

quasi-particle interactions, necessary for consistency!

# Landau-Fermi Liquid (II)

- quasi-particle occupation $\delta n_k$ :
  - adiabatically connected to ideal gas occupation
  - not directly observable
- parameters [m*, f(k,k)] at $k_F$ determined by few measurments
  (specific heat C, compressibility, magnetic susceptibility,...)

  $\Rightarrow$ predicitions

  for transport properties, ...

→ Limits of applicability?

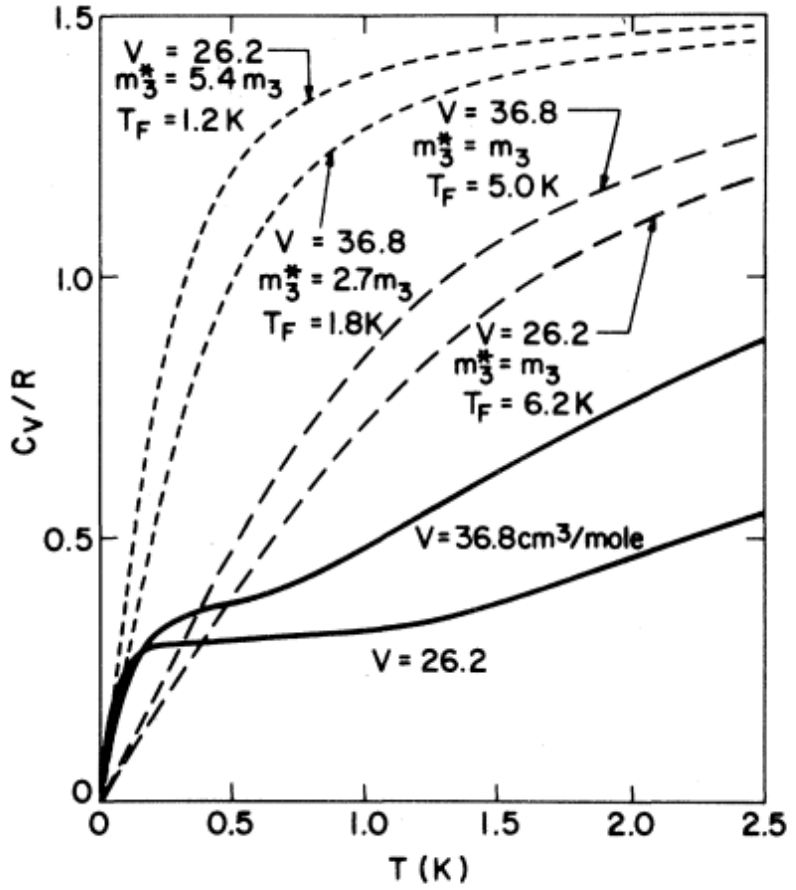


specific heat of liquid $^3He$

D. Greywall PRB 27, 2747 (1983)

# Fermi Liquid: Microscopic Description (I)

Single particle Green's function: $G_R(k,t) \equiv -i \left\langle e^{iHt} a_k e^{-iHt} a_k^\dagger \right\rangle \theta(t)$

$$= \int \frac{d\omega}{2\pi} G_R(k,\omega) e^{-i\omega t}$$

$$G_R(k,\omega) = \sum_n \frac{\left| \left\langle n | a_k^\dagger | 0 \right\rangle \right|^2}{\omega - (E_n^{N+1} - E_0^N - \mu) + i\eta}$$

excitation energies ➠ peaks in spectral function

$$A(k,\omega) = -\frac{1}{\pi} \mathrm{Im} G_R(k,\omega)$$ (measured in ARPES)

## ideal gas

$$A_0(k,\omega) = \delta(\omega - \mu - k^2/2m)$$

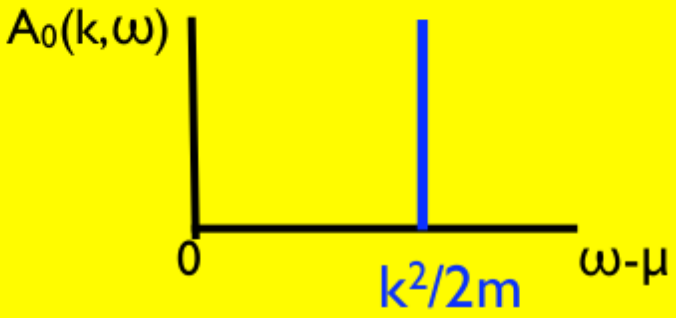


## interacting system

$$A_0(k,\omega) = \frac{Z_k}{2\pi} \frac{\tau_k^{-1}}{(\omega - \mu - \varepsilon_k)^2 + (2\tau_k)^{-2}} + A_{\mathrm{inc}}$$

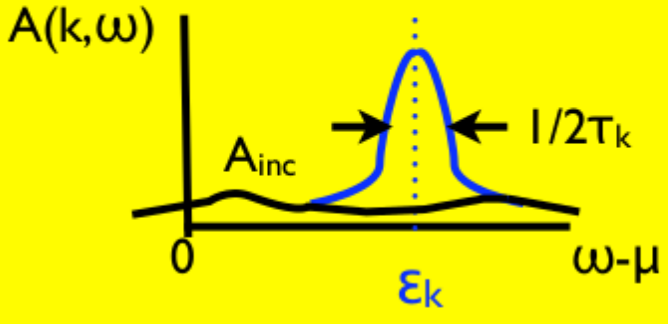

# Fermi Liquid: Microscopic Description (II)

Self-energy Σ(k,ω): $G^{-1}(k,\omega) = \omega - \mu - k^2/2m - \Sigma(k,\omega)$

form of G around quasi-particle peak $G^{-1}(k, \omega - \mu \approx \varepsilon_k) = Z_k^{-1}(\omega - \mu - \varepsilon_k + i\tau_k/2)$

quasi-particle energy: $\varepsilon_k = k^2/2m + \mathrm{Re}\,\Sigma(k, \mu + \varepsilon_k)$

inverse quasi-particle weight: $Z_k^{-1} = 1 - \partial \mathrm{Re}\,\Sigma(k, \mu + \varepsilon_k)/\partial\omega$

inverse lifetime: $\tau_k^{-1} = -2Z_k\,\mathrm{Im}\,\Sigma(k, \mu + \varepsilon_k)$

Definition of Fermi liquid: $\tau_k^{-1} \to 0 \quad \text{for} \quad k \to k_F$

Delta function excitation at the Fermi surface $A(k \to k_F, \omega \approx \mu) = Z_k \delta(\omega - \mu - k^2/2m^*)$

$m/m^* = Z_{k_F}\,(1 + m/k_F\,\partial\Sigma(k_F, \mu)/\partial k)$

with effective mass m* from expansion around $\omega - \mu = \varepsilon_k \equiv k^2/2m*$

$\Sigma(k, \mu + \varepsilon_k) = \Sigma(k_F, \mu) + (k - k_F)\partial\Sigma(k_F, \mu)/\partial k + \varepsilon_k \partial\Sigma(k_F, \mu)/\partial\omega + \ldots$

# Fermi Liquid: Momentum Distribution $n_k$

Sharp jump of $n_k$ at $k_F$ is consequence of δ-function excitation at $k_F$

$$n_k \equiv \langle a_k^\dagger a_k \rangle = \int_{-\infty}^{\mu} d\omega A(k,\omega)$$

$k<k_F$: quasi-particle peak of A below μ

$p>k_F$: quasi-particle peak of A above μ

$$n_k - n_p \simeq Z_k + \int_{-\infty}^{\mu} d\omega \left[A_{inc}(k,\omega) - A_{inc}(p,\omega)\right]$$

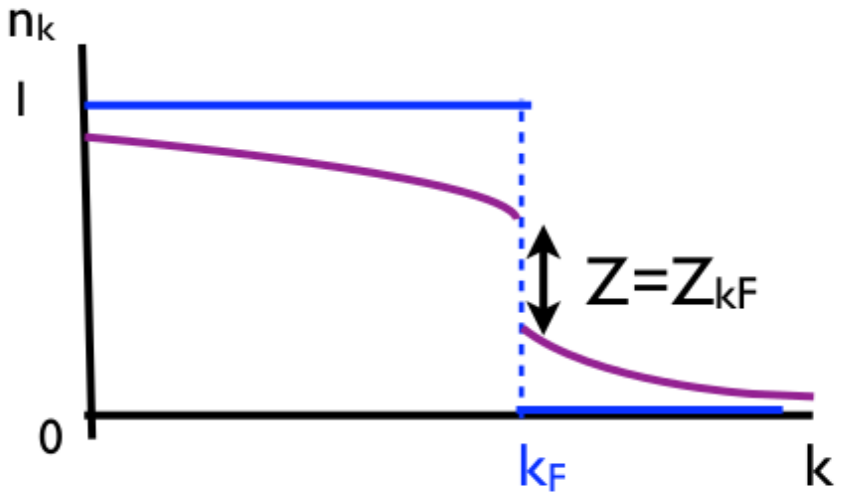

# n(k), Z of jellium (3DEG) at various densities

M.H., B. Bernu, C. Pierleoni, J. McMinis, D.M. Ceperley, V. Olevano, L. Delle Site, PRL **107**, 110402 (2011) (2011).

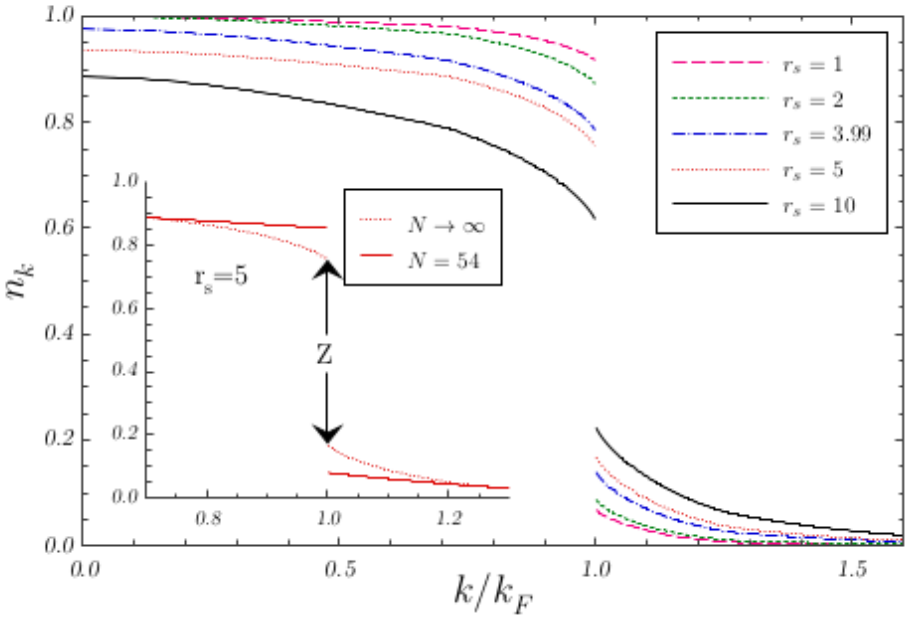


from analytical expressions of Ψ:
exact behavior of $n_k$ around $k_F$

Quantitative agreement of QMC with $G_0W_0$ over broad density region $1 \le r_s \le 5...10$)

| $r_s$ | 1 | 2 | 3.99 | 5 | 10 |
|---|---|---|---|---|---|
| BF-RMC | 0.84(2) | 0.77(1) | 0.64(1) | 0.58(1) | 0.40(1) |
| SJ-VMC | 0.894(9) | 0.82(1) | 0.69(1) | 0.61(2) | 0.45(1) |
| BF-VMC | 0.86(1) | 0.78(1) | 0.65(1) | 0.59(1) | 0.41(1) |
| $G_0W_0$ [25] | 0.859 | 0.768 | 0.646* | 0.602 | 0.45 |
| $GW_0$ [26] | | 0.804 | 0.702* | | |
| $GW$ [27] | | 0.846 | 0.793* | | |
| Lam [28] | 0.896 | 0.814 | 0.615* | 0.472 | |
| RPA [28] | 0.843 | 0.700 | 0.442* | 0.323 | |
| SJ-DMC [6] | 0.952 | 0.889 | | 0.725 | 0.593 |


[25] L. Hedin, Phys.Rev. 139, A796 (1965).
[26] U. von Barth, B. Holm, PRB 54, 8411 (1996).
[27] B. Holm, U. von Barth, PRB 57, 2108 (1998).
[28] J. Lam, PRB 3, 3243 (1971).
[6] G. Ortiz, P. Ballone, PRB 50, 1391 (1994).


## renormalization factor Z

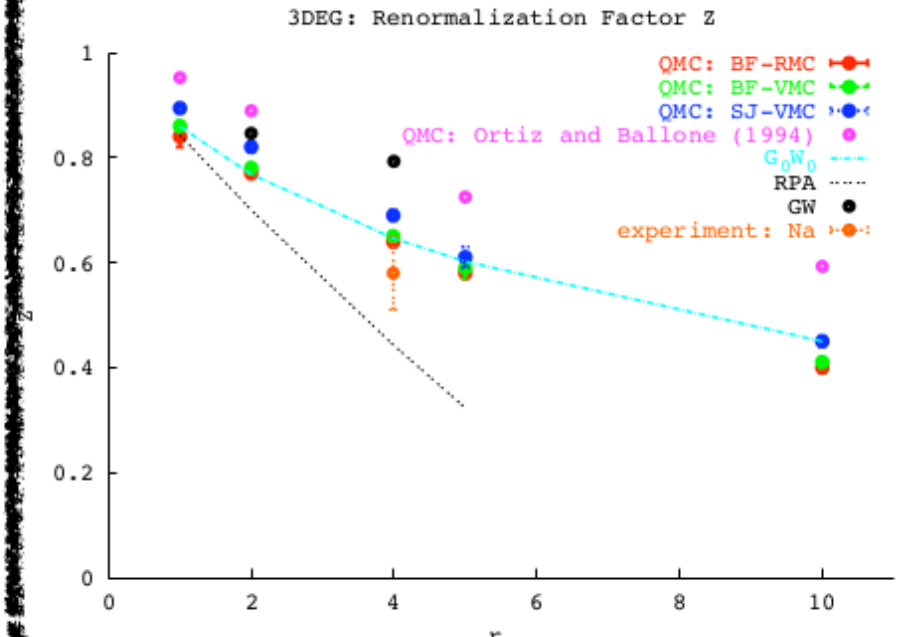

# Renormalization factor Z

Best QMC: BF-RMC

M. H., B. Bernu, C. Pierleoni, J. McMinis, D. M. Ceperley, V. Olevano, and L. Delle Site, Phys. Rev. Lett. 107, 110402 (2011).

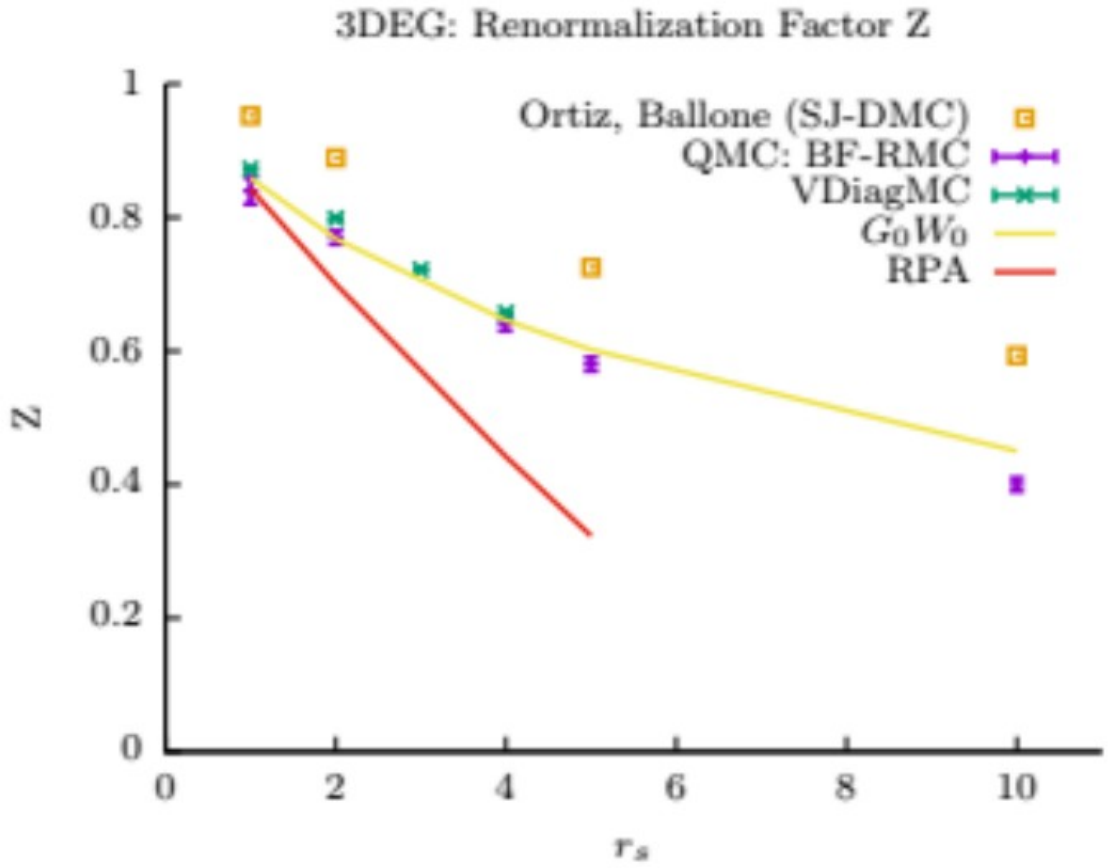


- Comparisons:
  - RPA
  - $G_0W_0$
  - beyond $G_0W_0$: Variational diagramatic Monte Carlo (VDiagMC)

K. Haule and K. Chen, Scientific Reports 12, 2294 (2022).

# Effective mass m*

- Controversy:
  VdiagMC,K. Haule and K. Chen,
  Scientific Reports 12, 2294 (2022)
  vs QMC study by
  Azadi, Drummond, Foulkes
  PRL 127, 086401 (2021)

- However:
  QMC based on assumptions
  for Landau energy functional
  VdiagMC based on Green's function

$$\delta E = \sum_{p\sigma} (\varepsilon_p + \mu)\delta n_{p\sigma} + \frac{1}{2V} \sum_{p\sigma, p'\sigma'} f(p\sigma, p'\sigma')\delta n_{p\sigma}\delta n_{p'\sigma'}$$

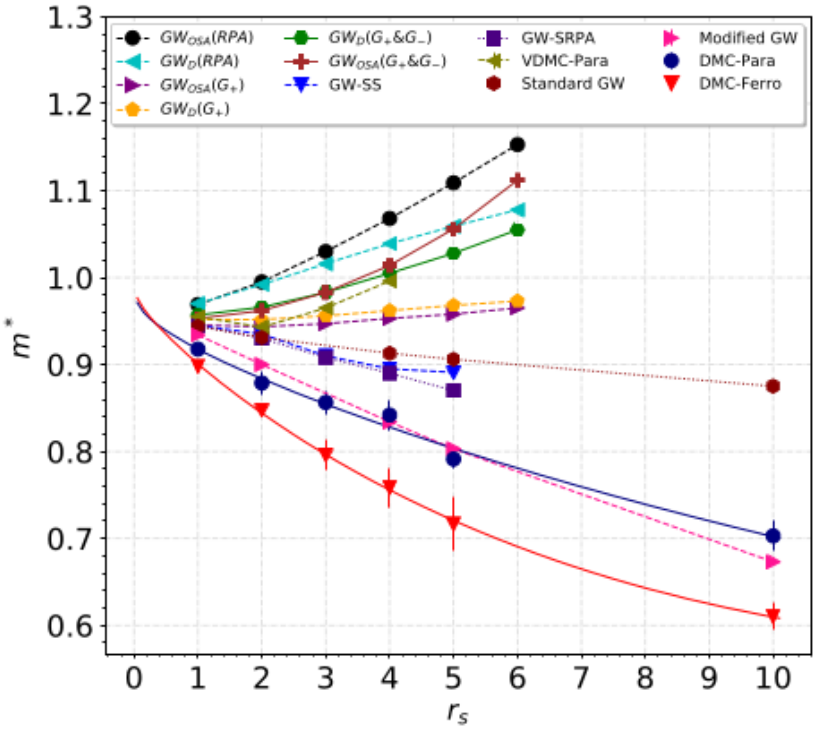


FIG. 4. Quasiparticle effective masses $m^*$ of paramagnetic (Para) and ferromagnetic (Ferro) 3D HEGs at the infinite-system-size limit as functions of density parameter $r_s$. Padé functions were fitted to the DMC quasiparticle energy bands to determine the effective mass. The many-body $GW_x$ and variational diagrammatic Monte Carlo (VDMC) results are from Refs. [52] and [53], respectively. The $GW$ SS and $GW$ SRPA results are from Refs. [54] and [55], respectively. The "standard $GW$" data and "modified $GW$" data are taken from Ref. [56]. All the $GW$ results are for paramagnetic 3D HEGs.

major problem with mapping of QMC trial-wave function to phenomenological Landau functional

$$E(\delta m_k) = E_0 + \sum_k \varepsilon_k^0 \delta m_k + \frac{1}{2V} \sum_{k\sigma k'\sigma'} f_{k\sigma,k'\sigma'} \delta m_k \delta m_{k'} + \ldots$$

definition of $\delta m_k$ only unique for lowest energy state with different total momentum

2 extrapolations:

- $N \to \infty$
- $k \to k_F$

≡ 2 major difficulties !

for any system size, N,
only very few states
close to the Fermi surface
can be used

(basically states with infinite lifetime!)

(does $N \to \infty$, $k \to k_F$ commute?)

➥need for new QMC methodology for m*

# Microscopic Definition of m*

Def. from single particle Green's function

$$\frac{m}{m^*} = \frac{1 + \frac{m}{k_F}\frac{\partial \Sigma(k_F,\mu)}{\partial k}}{1 - \frac{\partial \Sigma(k_F,\mu)}{\partial \omega}}$$

Fermi liquids have jump Z in momentum distribution:

$$Z = \frac{1}{1 - \frac{\partial \Sigma(k_F,\mu)}{\partial \omega}}$$

✘ we calculate Z within QMC

❑ how to calculate k-derivative of self-energy? $\frac{\partial \Sigma(k_F,\mu)}{\partial k}$

➥note that Σ(k,μ) is a static quantity

and G(k,μ) is a static response function!

# QMC calculation of the static self-energy (I)

## QMC can calculate static response function remaining variational

VOLUME 69, NUMBER 13 PHYSICAL REVIEW LETTERS 28 SEPTEMBER 1992

**Static Response from Quantum Monte Carlo Calculations**

Saverio Moroni,[1],[a] David M. Ceperley,[1] and Gaetano Senatore[2]
[1] *National Center for Supercomputing Applications and Department of Physics, University of Illinois at Urbana-Champaign, Urbana, Illinois 61801*
[2] *Dipartimento di Fisica Teorica, Università di Trieste, Strada Costiera 11, I-34014 Trieste, Italy*
(Received 18 June 1992)

$$v_{\mathrm{ext}}(\mathbf{r}) = 2v_{\mathbf{q}} \cos(\mathbf{q}\cdot\mathbf{r}),$$

$$E_v = E_0 + \frac{\chi(q)}{n_0} v_{\mathbf{q}}^2 + C_4 v_{\mathbf{q}}^4 + \cdots.$$

## adapt for single particle excitation:

add external potential $\xi$ $a_k^+$ to Hamiltonian $H(\xi_k) = H - \mu N + \xi_k a_k^\dagger + \xi_k^* a_k$

and minimize energy using N/N+1 wave function $E(\xi_k) - E_0 = G(k,\mu)\,\xi_k^2$

$\Rightarrow$ static self-energy $\Sigma(k,\mu) = \mu - G^{-1}(k,\mu) - k^2/2m$

# QMC calculation of the static self-energy (II)

$$H(\xi_k) = H - \mu N + \xi_k a_k^\dagger + \xi_k^* a_k$$

$$E_0(\xi_k) \leq \frac{\langle \Psi_k | H(\xi_k) | \Psi_k \rangle}{\langle \Psi_k | \Psi_k \rangle}$$

ansatz for wave function: $\Psi_k(\mathbf{R}) = \psi_0^N(\mathbf{R}_N) + \alpha_k \psi_k^{N+1}(\mathbf{R}_{N+1})$

$$E_0(\xi_k) = E_0 - \frac{z_k}{E_k^{N+1} - E_0^N - \mu} \xi_k^2, \quad \text{for } \xi_k \to 0$$

$$z_k = \frac{|\langle \psi^{N+1} | a_k^\dagger | \psi_0^N \rangle|^2}{\langle \psi_0^N | \psi_0^N \rangle \langle \psi_k^{N+1} | \psi_k^{N+1} \rangle} \qquad E_k^{N+1} = \frac{\langle \psi_k^{N+1} | H \psi_k^{N+1} \rangle}{\langle \psi_k^{N+1} | \psi_k^{N+1} \rangle}$$

chose wave function such that:

a) minimize energy difference $E_k^{N+1} - E_0^N - \mu$ $\quad \phi_k^{N+1}(\mathbf{R}_{N+1}) = \det_{ik} \varphi_k(\mathbf{q}_i) e^{-U_{N+1}}$

b) maximize overlap $z_k$ $\quad a_k^\dagger \psi_0^N(\mathbf{R}_N)$

# Static self-energy

M.H., F. Calcavecchia, D.M. Ceperley, V. Olevano, cond-mat 2305.02274 (2023)

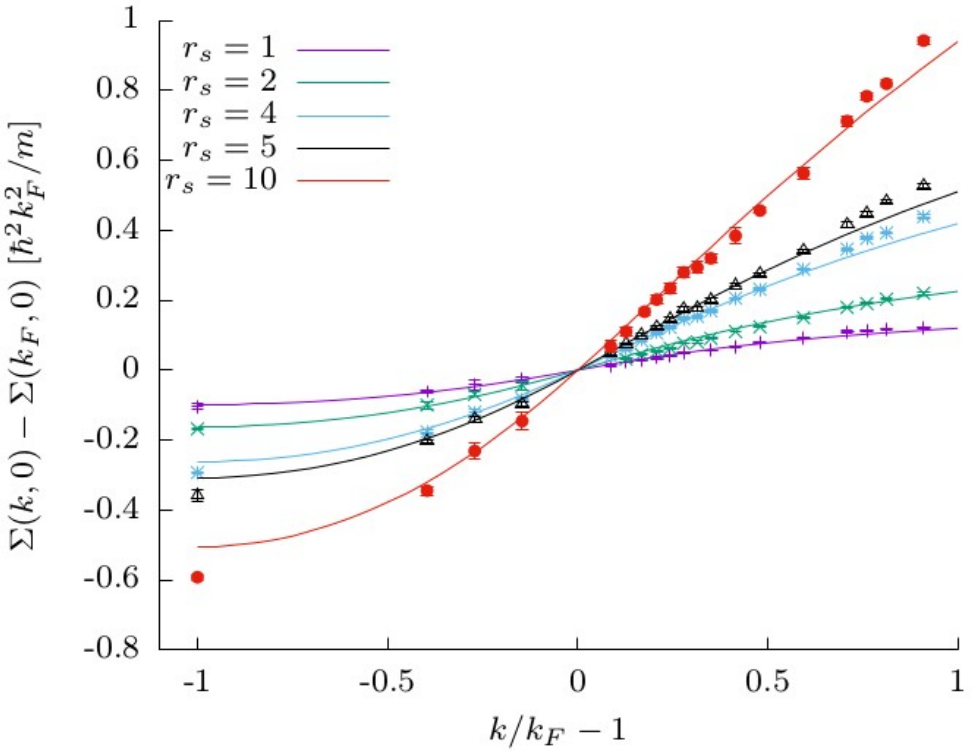


FIG. 1: Static self-energy for various densities ($r_s$) using backflow (BF) trial wave functions and GC-TABC simulations for $N = 38$ electrons. They include size corrections. The color lines are from $G_0W_0$ calculations.

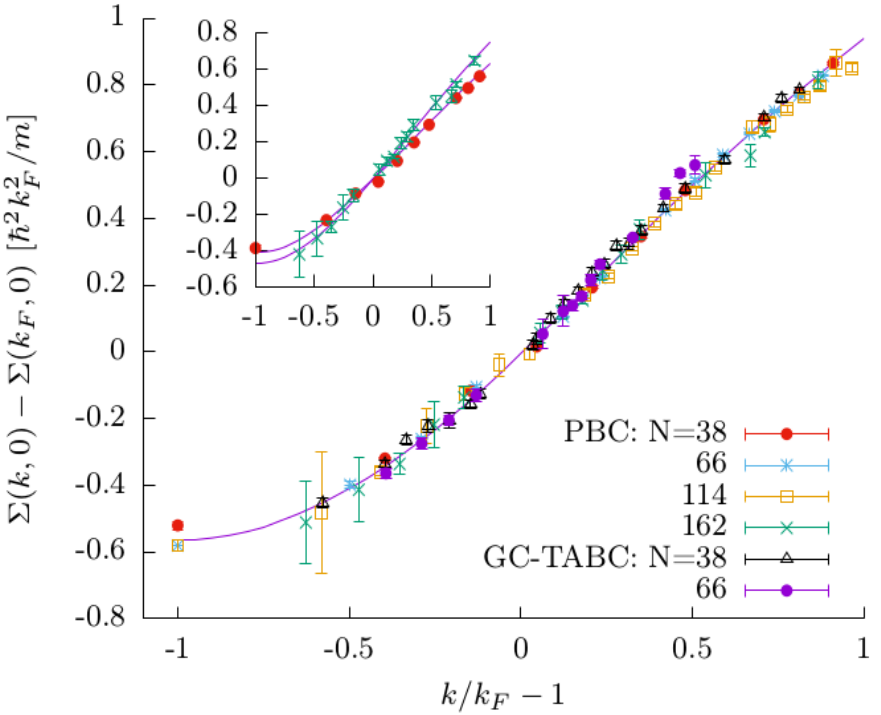


FIG. 2: Static self-energy for $r_s = 10$ using SJ-VMC trial wave functions for simulations with periodic boundary conditions (PBC) and GC-TABC for various sizes ranging from $N = 38$ to $N = 162$, size corrected according to Eq. (17), the line is a fit to the data. The inset shows the uncorrected values for $N = 38$ and $N = 162$ (PBC), the lines indicate the size corrections of the fit based on Eq. 17).

# Size corrections (analytic):

M. H., B. Bernu, D. Ceperley, J. Phys.: Conf. Ser. 321 012020 (2011), cond-mat/1105.2964.

*4.2. Renormalization factor and effective mass*

For the calculation of the renormalization factor and the effective mass, we need the derivatives of the self energy at the Fermi surface. Within the RPA, we have

$$\frac{\partial\Sigma(k_F,\varepsilon_F)}{\partial\omega} = -\frac{1}{V}\sum_{\mathbf{q}\neq 0}\int_{-\infty}^{\infty}\frac{d\nu}{(2\pi)}\left[\frac{1}{\epsilon(q,i\nu)}-\frac{1}{\epsilon(q,0)}\right]\frac{v_q}{[i\nu+\varepsilon_F-\varepsilon_{k_F+\mathbf{q}}]^2} \qquad (19)$$

$q\to 0$

$$\frac{m}{k_F}\frac{\partial\Sigma(k_F,\varepsilon_F)}{\partial k} = \frac{1}{V}\sum_{\mathbf{q}\neq 0}\int_{-\infty}^{\infty}\frac{d\nu}{(2\pi)}\frac{1}{\epsilon(q,i\nu)}\frac{v_q}{[i\nu+\varepsilon_F-\varepsilon_{k_F+\mathbf{q}}]^2}\left[1+\frac{\mathbf{k}_F\cdot\mathbf{q}}{k_F^2}\right] \qquad (20)$$

➡ Leading order size corrections from Coulomb singularity (q⟶0)

Exact (beyond RPA) leading order finite size corrections (based on Ward identities):

$$\delta\Sigma(k,0) \simeq -\int_{-\pi/L}^{\pi/L}\frac{d^3q}{(2\pi)^3}\int_{-\infty}^{\infty}\frac{d\nu}{(2\pi)}\frac{v_q}{\epsilon(q,i\nu)}\frac{1}{i\nu+\mu-\varepsilon^0_{k+q}}$$

# Z + static self-energy = m*

M.H., F. Calcavecchia, D.M. Ceperley, V. Olevano, cond-mat 2305.02274 (2023)

| $r_s$ | method | $Z$ | $mk_F^{-1}\partial_k\Sigma$ | $m^*/m$ |
|---|---|---|---|---|
| 1 | BF-VMC | 0.86(1) [13] | $0.17^{0.18}_{0.15}(1)$ | $1.00^{1.01}_{0.99}(1)$ |
| | SJ-VMC | 0.894(9) [13] | $0.17^{0.18}_{0.15}(1)$ | $0.96^{0.97}_{0.95}(1)$ |
| | $G_0W_0$ (RPA) | 0.859 [31] | 0.200 | 0.970 [10] |
| | VDiagMC [12] | 0.8725(2) | 0.200(1) | 0.955(1) |
| 2 | BF-VMC | 0.78(1) | $0.309^{0.361}_{0.280}(6)$ | $0.98^{1.00}_{0.94}(1)$ |
| | SJ-VMC | 0.82(1) | $0.30^{0.31}_{0.28}(2)$ | $0.94^{0.95}_{0.93}(2)$ |
| | $G_0W_0$ (RPA) | 0.768 [31] | 0.313 | 0.992 [10] |
| | VDiagMC [12] | 0.7984(2) | 0.328(4) | 0.943(3) |
| 4 | BF-VMC | 0.65(1) | $0.538^{0.549}_{0.530}(7)$ | $1.00^{1.01}_{0.99}(2)$ |
| | SJ-VMC | 0.69(1) | $0.55_{0.45}(2)$ | $0.94^{1.00}(2)$ |
| | $G_0W_0$ (RPA) | 0.646 [31] | 0.490 | 1.039 [10] |
| | VDiagMC [12] | 0.6571(2) | 0.528(5) | 0.996(3) |
| 5 | BF-VMC | 0.59(1) | $0.56^{0.65}(1)$ | $1.09_{1.03}(3)$ |
| | SJ-VMC | 0.61(1) | $0.610^{0.624}_{0.596}(9)$ | $1.02^{1.03}_{1.01}(2)$ |
| | $G_0W_0$ (RPA) | 0.602 [31] | 0.569 | 1.059 [10] |
| 10 | BF-VMC | 0.41(1) | $0.90^{0.98}_{0.88}(2)$ | $1.28^{1.30}_{1.23}(3)$ |
| | SJ-VMC | 0.45(1) | $0.97^{1.03}_{0.91}(3)$ | $1.13^{1.16}_{1.09}(3)$ |
| | $G_0W_0$ (RPA) | 0.45 [31] | 0.98 | 1.13 |

TABLE I: Our QMC results with backflow (BF) and Slater-Jastrow (SJ) trial functions as compared to those of $G_0W_0$ (RPA) and variational diagrammatic Monte Carlo (VDiagMC) [12, 32, 33]. Upper and low indices indicate systematic errors assuming different fitting functions/ranges to determine $\partial_k\Sigma(k_F, 0)$.

# Experimental realisations of jellium?
## valence electrons of alcaline metals

- Band structure:
  Na: almost isotropic
  Li: anisotropic
- Influence of Core electrons? (pseudo-potential vs all electron)
- Electron-phonon coupling?
- Temperature effects?
- Pressure: small variation of density, solid and liquid phases
- Direct probes and signes of electron correlations?

momentum distribution

# Momentum distribution of the homogeneous electron gas in 3D (3DEG): $G_0W_0$, QMC, experiment...

S. Huotari, J. A. Soininen, T. Pylkkänen, A. Titov, A. Issolah, K. Hämäläinen, J. McMinis, J. Kim, K. Esler, D.M. Ceperley, M. H., and V. Olevano, Phys. Rev. Lett. 105, 086403 (2010).

valence electrons in Na ≈ 3DEG

- Na: very isotropic valence band
- spherical Fermi surface: anisotropies around $k_F$ <≈0.2%

momentum distribution can be measured
via inelastic X-ray scattering
(Compton profile)

# Compton profile from inelastic X-ray scattering

scattering cross section:

$$\frac{d^2\sigma}{d\Omega d\omega_2} = \left(\frac{d\sigma}{d\Omega}\right)_{Th} S(\mathbf{k},\omega)$$

dynamic structure factor

high energies (synchrotron): impulsive approximation

$$S(\mathbf{k},\omega) \simeq J_{\hat{\mathbf{k}}}\left(\omega/k - k/2\right)$$

Compton profile

$$J_{\mathbf{k}}(q) = \int d^3\mathbf{p}\, n(\mathbf{p})\delta(\mathbf{p}\cdot\hat{\mathbf{k}} - q)$$

spherical averaged Compton profile

$$J(q) = \int_{|q|}^{\infty} d^2\mathbf{p}\, n(\mathbf{p})$$

momentum distribution n(k) by differentiation

renormalization factor Z gives kink

# Valence electron Compton profile of Na: experiment

subtract contribution of core electrons

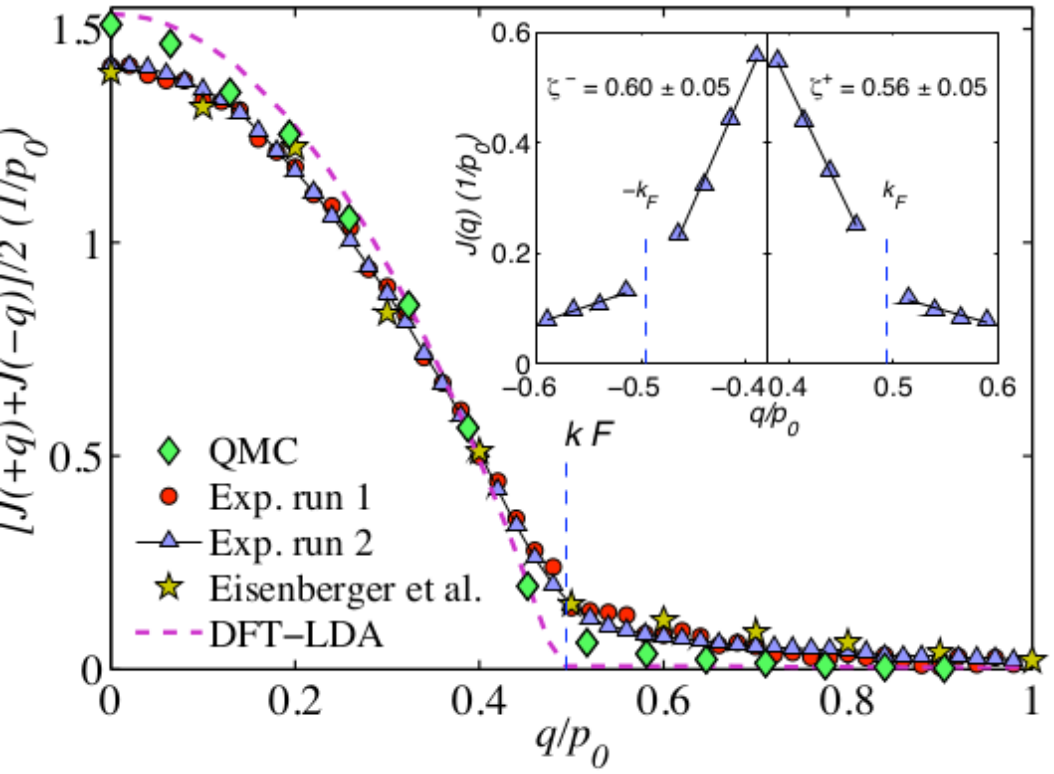


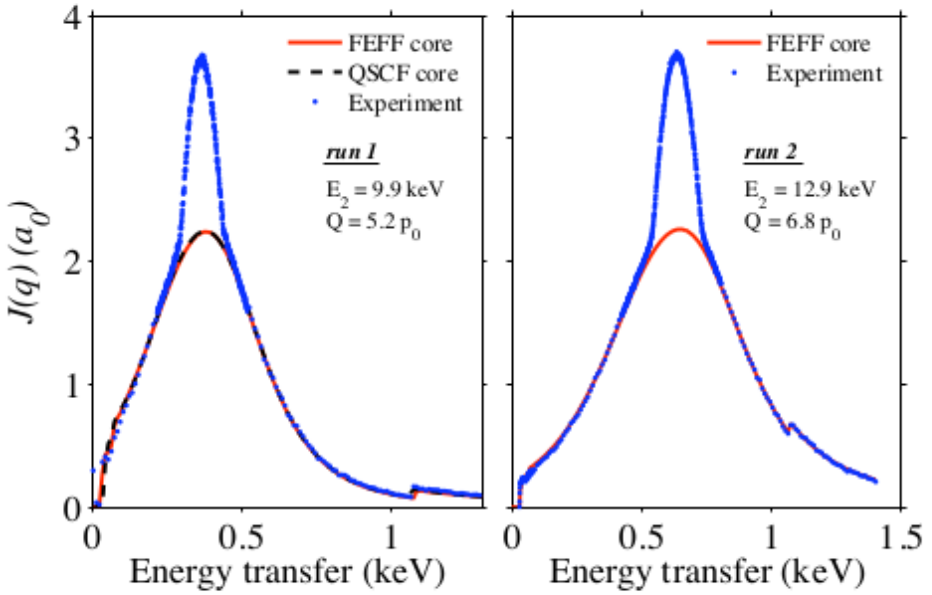


FIG. 2 (color online). The measured x-ray-scattering spectra from Na as a function of energy transfer, for both experimental runs. The experimental spectra consist of overlapping valence and core contributions. Theoretical core contributions are shown for both QSCF and FEFFQ treatments.

discontinuity in the slope at $k_F$: direct measurement of Z and $k_F$

# momentum distribution of Na
# renormalization factor Z of 3DEG at $r_s$=3.99

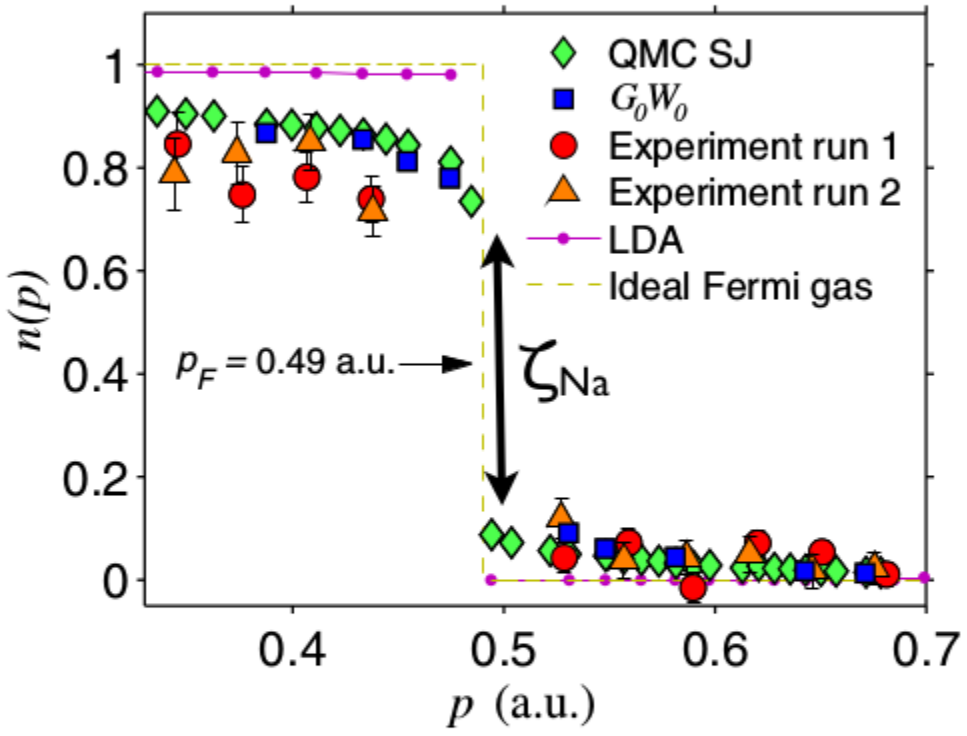


FIG. 1 (color online). The momentum distribution of Na determined by experiment, QMC SJ, $G_0W_0$, and LDA calculations. The ideal-Fermi gas step function is also shown.

valence electron density:
$r_s$=3.99

QMC and $G_0W_0$ indicate
that bandstructure and correlation effects
factorize at $k_F$

$$\zeta_{\mathrm{Na}} = |\tilde{\phi}^{\mathbf{G}=0}_{\nu=1,\mathbf{k}_F}|^2 Z_{\mathbf{k}_F}$$

LDA bandstructure wfn-coeff.

$Z_{Na} \cong Z_{3DEG}$

| Technique | $\zeta^{Na}$ | $Z^{Na}_{k_F}$ | $Z^{HEG}_{k_F}$ |
|---|---|---|---|
| Experiment | 0.57(7) | 0.58(7) | |
| QMC SJ | 0.68(2) | 0.70(2) | 0.69(1) |
| QMC BF | | | 0.66(2) |
| $G_0W_0$ | 0.64(1) | 0.65(1) | 0.64 [2] |
| $GW$ [6] | | | 0.793 |
| RPA (on shell) | | | 0.45 |
| exp$S_2$ [4] | | | 0.59 |
| EPX [8] | | | 0.61 |
| Lam [5] | | | 0.615 |
| FHNC [7] | | | 0.71 |

comparision with theories

# Momentum distribution of solid and liquid Li ($r_s$=3.25): Experiment vs QMC (full electron)

Yang, Hiraoka, Matsuda, M. H., Ceperley,
Phys. Rev. B 101, 165125 (2020);
Hiraoka, Yang, Hagiya, Niozu, Matsuda, Huotari, M. H., Ceperley,
Phys. Rev. B 101, 165124 (2020).

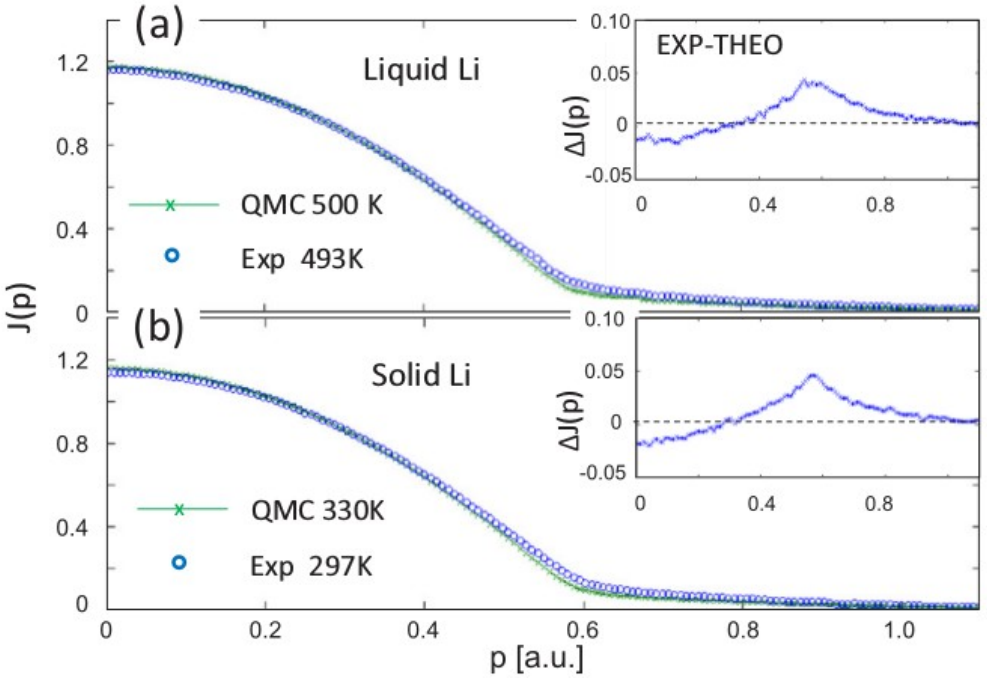


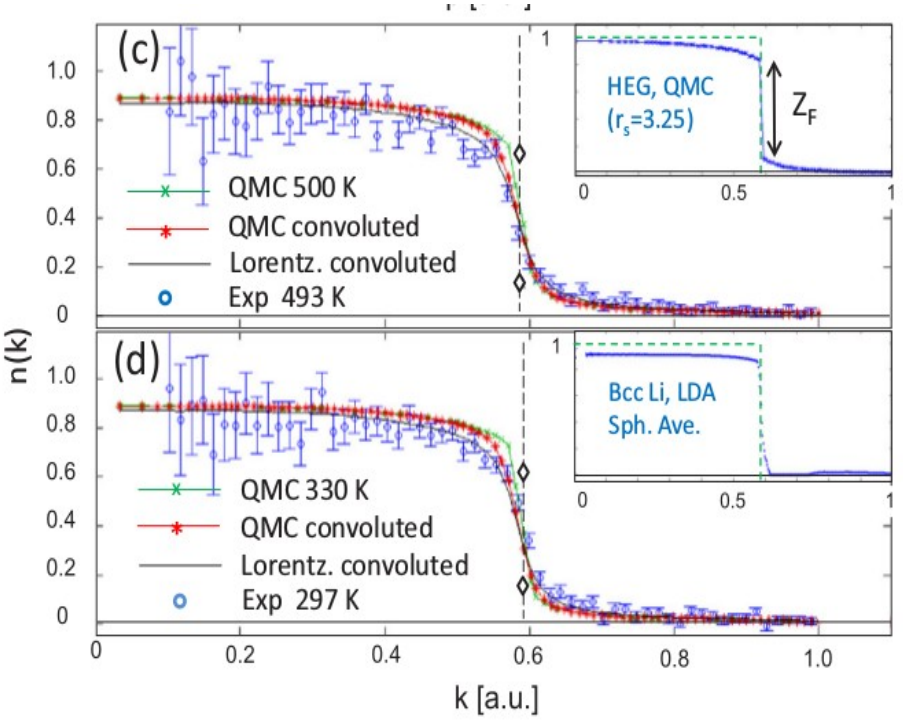


FIG. 2. Valance CPs of liquid (a) and solid Li (b), compared with theory convoluted by the broadening function. The insets show the difference between the experimental and theoretical CPs. EMDs in liquid (c) and solid Li (d), compared to theory with or without the convolutions. The insets show EMD for HEG and the spherically averaged EMD from band theory (LDA). The ◊'s in (c) and (d) show the $n(k_F)$ obtained by RPA fits near $k_F$.

# Summary - Conclusions:

- Improvement of ground state wave functions:
  iterated backflow, machine learned network ansätze...
- Jellium: many-body correlations supress polarization transition,
  true for all isotropic and spin-intependent interactions?
- Gaps: single particle and p-h excitations, size effects, S(k)….
- Fermi Liquid parameters: Z, m*

Vitaly Gorelov

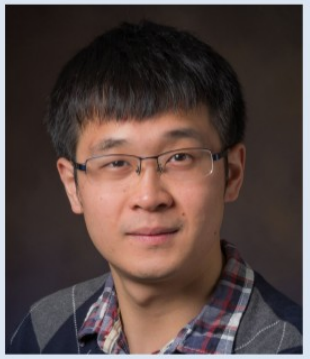

**Yubo Yang**
Flatiron

Saverio Moroni
(CNR, SISSA, Trieste)

Carlo Pierleoni
(University of L'Aquila)

Max Wilson
(DTU)

David Ceperley
(UIUC)

Valerio Olevano
(Néel, Grenoble)